Appl. Phys. B 91, 299–303 (2008)
DOI: 10.1007/s00340-008-2983-9

Applied Physics B
Lasers and Optics

V.A. LISINETSKII[1,✉]
V.A. ORLOVICH[1]
H. RHEE[2]
X. WANG[2]
H.J. EICHLER[2]

Efficient Raman amplification of low divergent radiation in barium nitrate crystal

[1] B.I. Stepanov Institute of Physics, NAS of Belarus, Nesalezhnasti Ave. 68, Minsk 220072, Belarus
[2] TU Berlin – Institut fuer Optik und Atomare Physik. Str. d. 17. Juni 135, 10623 Berlin, Germany

Received: 23 November 2007 /
Revised version: 11 February 2008
Published online: 27 March 2008 •

ABSTRACT One stage first Stokes amplification by a factor of 1600 was demonstrated in a barium nitrate Raman amplifier. The amplified pulse energy was up to 63 mJ at pump energy of 208 mJ. M^2 factor of Stokes signal radiation was 1.5 while for amplified radiation 2.2.

PACS 42.65.Dr

1 Introduction

Frequency conversion of laser radiation with stimulated Raman scattering (SRS) in solid-state media is of actual interest [1–15]. SRS allows one to decrease or to increase the laser radiation frequency by a discrete frequency of shift (Raman shift) equal to the frequency of a molecular vibration. This shift is fixed and provides stability of converted radiation frequency. SRS does not require any crystal angle tuning or strong temperature stabilization to stabilize the output radiation frequency.

Solid-state Raman media possess high concentrations (10^{22}–10^{23} cm^{-3}) of scattering centers and as a consequence high Raman gain coefficients. Together with good mechanical and thermal properties this allows one to use a small length Raman crystal. A typical Raman crystal length is of several centimeters; however, in some cases (Raman conversion of femtosecond [6] and picosecond [7] pulses, intracavity Raman conversion and self-frequency Raman conversion in diode pumped mini- [8] and microchip [9] lasers) a crystal of millimeter order length can be used. The Raman shift (700–1000 cm^{-1}) in widely used solid-state media [10, 11], being smaller than one in gases, increases the number of frequencies achievable by SRS. As a result, simple compact efficient Raman converters on the base of solid-state media for conversion of femtosecond [6], picosecond [12], nanosecond [1–5] and continuous wave [13] radiation were developed.

It is necessary in many applications (lidar, range-meters and so on) for frequency converted pulses to have a high energy and low divergence (low M^2 factor). Diffraction limited Stokes radiation with pulse energy of 250 mJ was generated with intracavity Raman conversion [3] (when Raman crystal is inserted in the laser cavity). However, the intracavity Raman conversion is unsuitable for conversion of commercial laser radiation, where Raman converters with external pumping are required.

Efficient conversion of high energy pulses of multimode commercial lasers was demonstrated in Raman lasers [5, 14, 15], when Raman medium is situated in external optical cavity. As compared with a single-pass scheme, Raman lasers possess a lower generation threshold, allow one to control the high-order Stokes generation and provide high efficiency of conversion into Stokes radiation of desired order. In [5] the generation of the first, second and third Stokes pulses with energies up to 156 mJ and with quantum efficiency up to 66% was demonstrated. However the M^2 factor of the converted radiation was about 20. The use of unstable telescopic cavity for Raman laser [15] allows one to decrease the M^2 factor down to 16, but this value is also very high.

Raman amplification is the alternative approach for Raman generation, which allows one to obtain high energy pulses. In spite of Raman generation when only a pump beam irradiates the Raman medium while Stokes radiation arises from noise, in Raman amplification pump and Stokes radiation are both incident on the Raman medium. The input Stokes radiation (Stokes signal) can be generated separately in a special Raman generator or an additional laser with the corresponding wavelength. Raman amplification was well studied before in gases [16–19]. It was shown, that when a low divergent Stokes signal radiation is used the amplified Stokes radiation also has a low divergence. The two stage amplification of Stokes pulses by a factor of 20 000 (amplified Stokes energy was about 0.6 J) was demonstrated [16]. The M^2 factor of amplified radiation was 1.1. In this work we demonstrate that Raman amplification in solid-state Raman media also allows one to generate high energy pulses with a low M^2 factor. A barium nitrate crystal was chosen as a Raman medium. This crystal possesses a very high value of Raman gain coefficient among crystals (10 cm/GW a 1064 nm wavelength [20]) and is a good choice for Raman amplification.

2 Experimental setup

The experimental setup is shown in the Fig. 1. We used a multimode commercial Nd:YAG laser (model

✉ Fax: +375-17-284-16-65, E-mail: lisinetskii@gmail.com

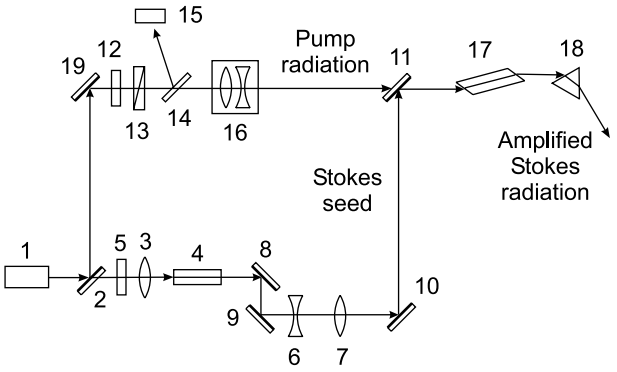

FIGURE 1 Experimental setup: (1) Nd:YAG laser, (2) beam splitter, (3) focusing lens, (4) barium nitrate crystal, (5) neutral filters, (6) concave lens, (7) convex lens, (8)–(11) selective mirrors, (12) half-wave plate, (13) polarizer, (14) beam splitter, (15) energy meter, (16) 3 × telescope, (17) barium nitrate crystals, (18) prism, (19) mirror

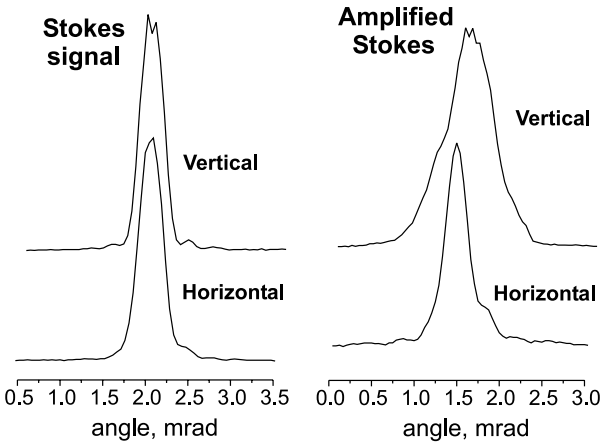

FIGURE 3 Horizontal and vertical profiles of Stokes signal and amplified Stokes beams. Stokes signal energy is 8 μJ

Spectraphysics DCR 3) (1) as a pump source. The laser operated in active Q-switch mode and generated pulsed radiation with a repetition rate of 20 Hz and pulse duration of 10 ns. The laser radiation wavelength was 1.064 μm, the spectral bandwidth was less than 0.8 cm^{-1}. The spectral width of pump radiation was measured with a HP 70950B optical spectrum analyzer with a HP 70004A display. The generated output beam had a diameter of 10 mm and M^2 factor of 3. The far-field intensity distribution of pump beam is shown in Fig. 2.

The pump radiation was divided by a beam splitter (2) in two parts. The first part with a small energy (about 2 mJ) was directed to the Raman generator. The Raman generator consisted of a focusing lens (3) and a barium nitrate crystal (4). The focusing lens (3) had a focal length of 200 mm. It focused pump radiation into the center of the barium nitrate crystal (4). The length of the barium nitrate crystal was 7 cm. Its facets were antireflection coated in the spectral region from 1.0 to 1.4 μm. The pump energy input to the Raman generator was controlled with neutral filters (5). The output Stokes radiation was collimated by a telescope consisting of a concave lens (6) with a focal length of 100 mm and a convex lens (7) with a focal length of 300 mm. A quite strong focusing of pump radiation into the barium nitrate crystal provides a small value of the Fresnel number for Raman generation. In this pump geometry the generation of small divergent Stokes radiation was achieved because of Raman beam clean-up [19]. This resulted in a nearly diffraction limited beam (M^2 factor was about 1.5) of generated first Stokes radiation. The vertical and horizontal profiles of this radiation are presented in Fig. 3a. The Raman generator operated quite far from Raman threshold to provide stability of parameters (energy, pulse duration) for the first Stokes radiation, and the second Stokes generation was weak enough to avoid instabilities of the first Stokes radiation related with this generation. We investigated two regimes for the Raman generator. In the first one the energy of the Stokes signal pulses incident on the Raman amplifier was 8 μJ, while in the second one this energy was 190 μJ.

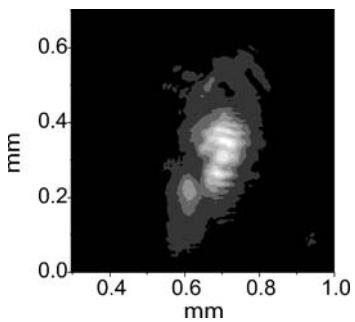

FIGURE 2 Far-field distribution of pump beam

The first Stokes radiation generated in the Raman generator was separated from depleted pump and the second Stokes radiation with four selective mirrors (8)–(11). Mirrors (8) and (9) had a high reflectivity at pump and the first Stokes wavelengths and low reflectivity at the second Stokes wavelength, while mirrors (10) and (11) had a high reflectivity at the first Stokes wavelength and a low reflectivity at pump wavelength. The selective mirror (11) was used also to combine the first Stokes radiation (Stokes signal) generated in the Raman generator with the second part of the pump beam reflected from the beam splitter (2).

The energy of pulses for second part of pump was controlled by the optical system consisting of a half-wave phase plate (12) and polarizer (13). The beam splitter (14) directed a part of pump radiation to the Soliton ED-200 energy meter (15) to measure the pump energy. The 3 × telescope (16) was used to decrease the pump beam diameter.

A 7 cm long barium nitrate crystal (17) was used for Raman amplification. The facets of the crystal were cut at Brewster angle to avoid feedback and prevent a decrease of the threshold for Raman generation in this crystal. The set of three prisms was used to separate amplified first Stokes radiation from the depleted pump radiation. The energies of Stokes signal and amplified Stokes pulses were measured with the Soliton ED-200 energy meter.

The optical path lengths for all radiations were chosen in such a way that Stokes signal and pump pulses were properly overlapped in time in the Raman amplifier. The oscilloscope traces of the input pump and Stokes pulses are presented in Fig. 4. The good overlap of pulses is evident. Figure 4 shows also that the Stokes signal pulse duration is nearly equal to the duration of the pump pulse. This indicates that the generation in Raman generator was far above the Raman threshold. All

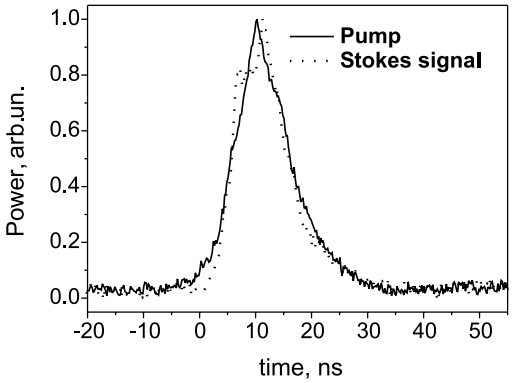

FIGURE 4 Oscilloscope traces of pump and Stokes signal pulses input to the Raman amplifier

of the oscilloscope traces in experiment were measured with two channel digital real-time oscilloscope Tektronix TDS 680B connected with fast photodiodes for IR measurements. The beams of Stokes signal and pump radiation were also matched. The measurements of spatial properties of pump radiation were performed with a silicon CCD camera (Polytec DVC 10) with a pixel size of 8.5×9.9 μm, while the measurements of first Stokes were performed with the use of InGaAs CCD array (Hamamatsu G 9204-512D) with pixel width of 25 μm.

In our experiments, we used pump pulses with energy not higher than 215 mJ. The threshold of direct Raman generation from noise in the Raman amplifier was about 250 mJ. Thus in our experiments only Raman amplification occurred.

3 Results and discussion

The dependencies of Stokes energy amplifications (ratio of amplified Stokes energy to Stokes signal energy) on pump energy for input Stokes pulses with energies of 8 μJ and 190 μJ are shown in the Fig. 5a. It is seen that amplification of Stokes pulses with energy of 8 μJ was up to 1600 at pump pulse energy of 215 mJ, while the amplification of Stokes pulses with energy of 190 μJ was up to 330 at pump pulse energy of 208 mJ. It is well known that the dependence of Stokes intensity on pump intensity in linear regime (when pump depletion is negligible) is exponential [21]:

$$I_S = I_{S0} \exp(I_P g L), \tag{1}$$

where I_S, I_{S0}, I_P – intensities of output Stokes, Stokes signal and pump intensities, g – steady-state Raman gain coefficient, L – Raman crystal length.

It follows from (1) that the natural logarithm of amplification can be expressed as:

$$\ln\left(\frac{I_S}{I_{S0}}\right) = G = I_P g L, \tag{2}$$

where G – steady-state power gain coefficient [22]. The Raman crystal length and pump radiation parameters (duration of 10 ns and beam diameter of 3 mm) used in experiments give the value for G equal to 21 for pump energies of 208–215 mJ, while the logarithm of Stokes energy amplification obtained in experiments at this pump energy was sufficiently lower:

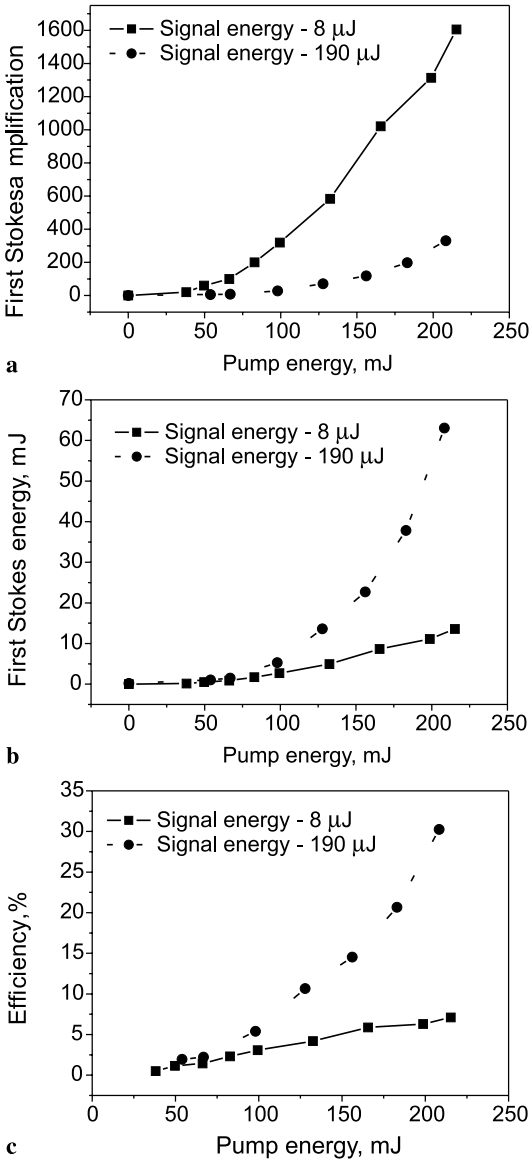

FIGURE 5 The dependencies of the first Stokes amplification (**a**), of amplified Stokes energy (**b**) and of conversion efficiency (**c**) on the pump pulse energy

only 7.4 for energy of Stokes signal pulses of 8 μJ and 5.8 for energy of Stokes signal pulses of 190 μJ. This is because pump and Stokes signal radiation used in experiments were not continuous wave and plane wave radiations. They possessed temporal and spatial shapes and an averaging of the steady-state power gain coefficient over space and time is required.

We considered the case when both pump and Stokes radiations possess a Gaussian shape in space and time:

$$I_{P,S0}(r,t) = \frac{E_{P,S0}}{\pi\sqrt{\pi} t_{P,S0} r_{P,S0}^2} \exp\left(-\left(\frac{r}{r_{P,S0}}\right)^2 - \left(\frac{t}{t_{P,S0}}\right)^2\right), \tag{3}$$

where E_P and E_{S0} – are energies of input pump and Stokes signal pulses, t_P and t_{S0} – durations of these pulses, r_P and r_{S0} – radii of input pump and Stokes signal beams, correspondingly.

The dependence of output Stokes intensity can be expressed as [21]:

$$I_{\mathrm{S}}(r,t) = \frac{\left(\frac{\omega_{\mathrm{S}}}{\omega_{\mathrm{P}}} I_{\mathrm{P}}(r,t) + I_{\mathrm{S0}}(r,t)\right) \exp\left(gL\left(\frac{\omega_{\mathrm{P}}}{\omega_{\mathrm{S}}} I_{\mathrm{S0}}(r,t) + I_{\mathrm{P}}(r,t)\right)\right)}{\frac{\omega_{\mathrm{S}}}{\omega_{\mathrm{P}}}\frac{I_{\mathrm{P}}(r,t)}{I_{\mathrm{S0}}(r,t)} + \exp\left(gL\left(\frac{\omega_{\mathrm{P}}}{\omega_{\mathrm{S}}} I_{\mathrm{S0}}(r,t) + I_{\mathrm{P}}(r,t)\right)\right)}, \tag{4}$$

where ω_{P} and ω_{S} – pump and Stokes frequencies. The saturation of amplification due to pump depletion is included also in this equation in contrast to (1). The equation is valid for a high Fresnel number of the amplifier (so-called ray-optics limit), where Fresnel number is [17]:

$$F = \frac{r_{\mathrm{P}}^2}{\lambda_{\mathrm{P}} L}, \tag{5}$$

with λ_{P} – pump wavelength.

In experiment the Fresnel number was equal to 30 and (4) is valid. The energy of amplified Stokes radiation can be obtained by integration of output Stokes intensity in space and time:

$$E_{\mathrm{S}} = \int_{-\infty}^{+\infty}\int_{0}^{\infty} I_{\mathrm{S}}(r,t)\, 2\pi r \,\mathrm{d}r\,\mathrm{d}t\,. \tag{6}$$

At parameters of the pump and Stokes signal radiation close to experimental ones (diameter – 3 mm, pulse duration – 10 ns, pump energy of 215 mJ for Stokes signal pulses with energy of 8 μJ and 208 mJ for Stokes signal pulses with energy of 190 μJ) we obtained values of G equal to 7.4 (amplification of 1650) for Stokes signal pulses with energy of 8 μJ and 5.4 (amplification of 222) for Stokes signal pulses with energy of 190 μJ. These values are in a good agreement with experimental ones.

The lower value of amplification for Stokes signal pulses with higher energy (190 μJ) as compared with 8 μJ Stokes signal pulses is related with saturation of Raman amplification due to pump depletion. Indeed, in spite of smaller amplification the energy of amplified pulses and conversion efficiency for Stokes signal pulses with energy of 190 μJ are five times higher than for Stokes signal pulses with energy of 8 μJ. Figures 5b and c show the dependencies of amplified Stokes energies and conversion efficiencies on pump energy. It is seen that for 190 μJ Stokes signal pulses the amplified Stokes energy was 63 mJ at pump energy of 210 mJ, which corresponds to the conversion efficiency of 30% (quantum conversion efficiency is 34%). For 8 μJ Stokes signal pulses the amplified Stokes energy was about 14 mJ, which corresponds to the conversion efficiency of 6% (quantum efficiency – 7%). Therefore high Stokes signal pulse energies are preferable to low pulse energies with higher amplification.

The efficient conversion of pump pulse energy into Stokes pulse energy led to significant pump depletion. Figure 6 shows oscilloscope traces of input and depleted pump pulses for amplification of Stokes signal pulses with energy of 8 μJ and for amplification of 190 μJ Stokes signal pulses. It is seen, that in the first case the depletion is very small, because of low conversion efficiency (only 6%), while in the second case this depletion is significant, because of 30% conversion efficiency. Figure 6 shows that depletion becomes apparent as slight decrease of the top of the pump pulse. This is because this figure demonstrates the oscilloscope trace of pump power (not intensity), where the nondepleted sides of pump beam are included. We have performed calculations of depleted pump intensity (I_{Depl}) using the Manley–Rowe relation [21]:

$$I_{\mathrm{Depl}}(r,t) = I_{\mathrm{P}}(r,t) - \left(I_{\mathrm{S}}(r,t) - I_{\mathrm{S0}}(r,t)\right)\frac{\omega_{\mathrm{P}}}{\omega_{\mathrm{S}}}\,. \tag{7}$$

Figure 7a shows the dependencies of intensities for input and depleted pump pulses in the middle of pump beam on time, calculated for Stokes signal pulses with energy of 190 μJ. It is seen that depletion in middle of pump pulse is strong. Figure 7b shows the calculated dependencies of powers for input and depleted pump pulses on time for these conditions (the power of depleted pump radiation was calculated by integration of depleted intensity in space). It is evident that the dependence for depleted pump is similar to the one presented in Fig. 6b.

The amplified Stokes beam was quite smooth both in the case of 8 μJ Stokes signal pulses and 190 μJ Stokes signal

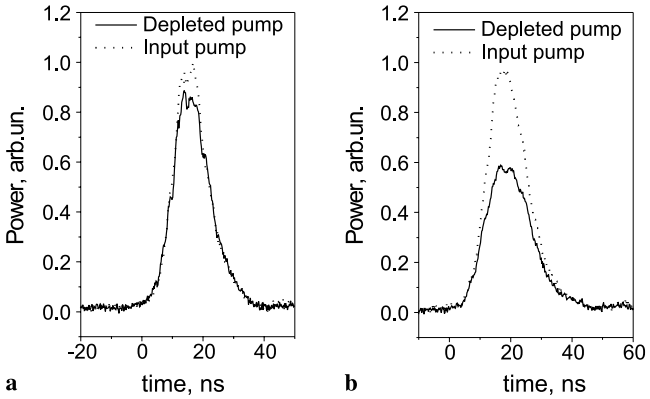

FIGURE 6 Oscilloscope traces of depleted and input pump pulses for Stokes signal pulses with energies of 8 μJ (**a**) and 190 μJ (**b**)

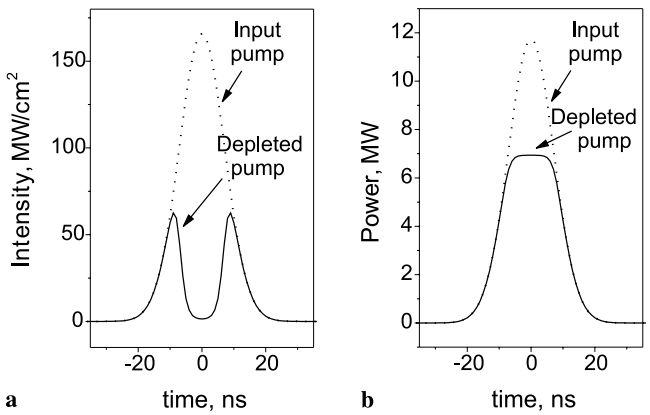

FIGURE 7 Calculated dependencies of intensities (**a**) and powers (**b**) of depleted and input pump pulses on time

pulses. Figure 3 demonstrates the horizontal and vertical profiles of amplified Stokes radiation measured at maximal pump energy. The M^2 factor of amplified Stokes beam was about 2, which is lower than M^2 factor of pump radiation. Thus the improvement of beam quality occurred during the Raman amplification in barium nitrate crystal.

We have also estimated using (4) and (6) the possibility of further amplification of the first Stokes radiation obtained in our experiment. It is possible to amplify the Stokes pulses with energy of 63 mJ up up to 350 mJ at pump pulse energy of 500 mJ. The Stokes and pump beam diameters were taken to be 5 mm, which allows one to avoid Raman generation in amplifier.

4 Conclusion

The efficient amplification of low divergent first Stokes radiation at multimode pumping was demonstrated. The energy of amplified pulses was up to 63 mJ at pump energy of 208 mJ, which corresponds to a quantum efficiency of 34%. The maximal amplification was 1600. Our estimations show that the second stage Raman amplification of amplified pulses up to 350 mJ is possible at pump pulse energy of 500 mJ. The improvement of beam quality in Raman amplification was demonstrated. The M^2 factor of amplified Stokes radiation was 2, compared to an M^2 factor of the pump radiation of 3.

REFERENCES

1 A.S. Eremenko, S.N. Karpukhin, A.I. Stepanov, Sov. J. Quantum Electron. **10**, 113 (1980)
2 S.N. Karpukhin, A.I. Stepanov, Sov. J. Quantum Electron. **16**, 1027 (1986)
3 J.T. Murray, R.C. Powell, N. Peyghambarian, D. Smith, W. Austin, R.A. Stolzenberger, Opt. Lett. **20**, 1017 (1995)
4 P.G. Zverev, T.T. Basiev, A.M. Prokhorov, Opt. Mater. **11**, 335 (1999)
5 V.A. Lisinetskii, A.S. Grabtchikov, I.A. Khodasevich, H.J. Eichler, V.A. Orlovich, Opt. Commun. **272**, 509 (2007)
6 A.S. Grabtchikov, R.V. Chulkov, V.A. Orlovich, M. Schmitt, R. Maksimenko, W. Kiefer, Opt. Lett. **28**, 926 (2003)
7 A.S. Grabtchikov, A.G. Shvedko, R.V. Chulkov, V.A. Lisinetskii, P.A. Apanasevich, V.A. Orlovich, in: 15th Int. Conf. Lasers and Electrooptics in Europe, Munich, Germany, June 18–22 2001, Conference Digest, Munich (2001), C-NLP219, p. 206
8 A.A. Demidovich, A.S. Grabtchikov, A.N. Kuzmin, V.A. Lisinetskii, V.A. Orlovich, Eur. Phys. J. Appl. Phys. **19**, 113 (2002)
9 A.A. Demidovich, P.A. Apanasevich, L.E. Batay, A.S. Grabtchikov, A.N. Kuzmin, V.A. Lisinetskii, V.A. Orlovich, O.V. Kuzmin, V.L. Hait, W. Kiefer, M.B. Danailov, Appl. Phys. B **76**, 509 (2003)
10 J. Hulliger, A.A. Kaminskii, H.J. Eichler, Adv. Funct. Mater. **11**, 243 (2001)
11 T.T. Basiev, A.A. Sobol, P.G. Zverev, L.I. Ivleva, V.V. Osiko, R.C. Powel, Opt. Mater. **11**, 307 (1999)
12 P. Cerny, H. Jelinkova, Opt. Lett. **27**, 360 (2002)
13 A.S. Grabtchikov, V.A. Lisinetskii, V.A. Orlovich, M. Schmitt, R. Maksimenka, W. Kiefer, Opt. Lett. **29**, 2524 (2004)
14 C. He, T.H. Chyba, Opt. Commun. **135**, 273 (1997)
15 V.V. Ermolenkov, V.A. Lisinetskii, I.I. Mishkel, A.S. Grabtchikov, A.P. Chaikovsky, V.A. Orlovich, J. Opt. Technol. **72**, 32 (2005)
16 A. Mandl, R. Holmes, A. Flusberg, S. Fulghum, D. Angeley, J. Appl. Phys. **66**, 4625 (1989)
17 C. Duzy, D. Korff, A. Flusberg, J. Daugherty, IEEE J. Quantum Electron. **QE-23**, 569 (1987)
18 H. Komine, W.H. Long, E.A. Stappaerts, S.J. Brosnan, J. Opt. Soc. Am. B **3**, 1428 (1986)
19 J. Reintjes, R.H. Lehmberg, R.S.F. Chang, M.T. Duilgnan, G. Calame, J. Opt. Soc. Am. B **3**, 1408 (1986)
20 V.A. Lisinetskii, I.I. Mishkel, R.V. Chulkov, A.S. Grabtchikov, P.A. Apanasevich, H.-J. Eichler, V.A. Orlovich, J. Nonlinear Opt. Phys. Mater. **14**, 107 (2005)
21 A. Penzkofer, A. Laubereau, W. Kaiser, Prog. Quantum Electron. **6**, 55 (1979)
22 R.L. Carman, F. Shimizu, C.S. Wang, N. Bloembergen, Phys. Rev. A **2**, 60 (1970)